

# Flight Effects on Fan Noise with Static and Wind-Tunnel Comparisons

John S. Preisser\* and David Chestnutt†  
*NASA Langley Research Center, Hampton, Virginia*

A flight test program utilizing a JT15D 1 turbofan engine has been conducted with the objective of studying flight effects on fan noise and evaluating the simulation effectiveness of both a wind tunnel and a static test configuration incorporating an inlet control device (ICD). In conjunction with synchronized laser radar tracking and meteorological profile information, data obtained from a linear array of ground microphones were narrowband analyzed and ensemble averaged to yield highly accurate far field flight acoustic results. Utilizing appropriate corrections, flight, wind tunnel, and static acoustic data were normalized to a static equivalent, 100 ft radius, lossless reference condition. Data comparisons showed that both the static test with ICD and wind tunnel were generally very effective in simulating flight blade passage frequency (BPF) noise levels. However, differences were observed in broadband noise levels and in the details of the multiple pure tone harmonics.

## Introduction

OVER the past decade considerable progress has been made in understanding the causes of the measured differences between static and flight turbofan inlet noise and in developing effective means for simulating flight noise in static tests. Experimental and analytical studies<sup>1,2</sup> had identified atmospheric turbulence, ground vortices, and test stand structure wakes as being primarily responsible for the strong blade passage frequency (BPF) tone that propagated at all power settings (including those with cut off rotor/stator interaction) during ground tests and which did not occur in flight. In recent years large spherical shaped honeycomb/screen structures have been developed by both industry and government for placement over turbofan inlets during static tests to simulate the flight flowfield environment, thereby reducing the tone noise arising from inflow disturbances.<sup>3,7</sup>

Simultaneous with the development of these structures the use of wind tunnels to achieve adequate flight simulation of fan noise was also being investigated. Effects of forward speed, angle of attack and advanced inlet design have been addressed in the Ames 40 × 80 ft Wind Tunnel, for example.<sup>8,12</sup> Results have shown that this simulation technique is also effective in reducing inflow distortion noise.

Comprehensive systematic studies, aimed at quantifying the effectiveness of inlet control devices (ICD's) and wind tunnels in flight noise simulation, are rare. In the only other known program,<sup>4,7,13</sup> flight data from a heavily instrumented JT9D 7 engine have been compared with ground test data utilizing two ICD (referred to as ICS's, inflow control structures therein) designs. Results from fan blade pressure transducers, in duct wall measurements, and one third octave far field acoustics indicated effective flight noise simulation was achieved by both designs. Differences between flight and static projected effective perceived noise levels were no larger than 1.6 EPNdB over a range of engine power settings. PNLT time histories, however, showed much larger (up to 7 dB) differences for some radiation angles. These comparisons included projected noise from multiple engines as well as aft

radiated fan noise, jet noise, and airframe noise. It is not certain whether the observed differences were due to inadequate projection of either these additional noise sources or the inlet radiated fan noise in question.

The present paper is concerned with a NASA intercenter research program that had the objective of further developing the understanding and techniques necessary for proper ground simulation of fan noise in flight. The program involved four NASA Centers: Langley, Lewis, Ames and Wallops. It involved testing similar heavily instrumented JT15D 1 turbofan engines on a static test stand (with and without ICD), in a wind tunnel, and in flight. Use of the same type engine and identical inlet lips enabled better comparison between results. A compact inlet control device designed by the Lewis Research Center<sup>6</sup> was used for the static part of the comparison. Wind tunnel results were taken from those published in Ref. 12. The present paper will discuss the technique and present results from flight tests involving the JT15D, including acoustic comparisons with the static and wind tunnel tests. Consideration will be given to separating the inlet radiated fan noise from the other noise sources and also, to identifying the particular fan noise sources which dominate in flight. All testing, including flight, is for a single engine in order to eliminate effects due to multiple engines. All far field acoustic results were analyzed in narrowband (100 Hz bandwidth) in order to effect a more critical evaluation.

## Test Description

### Engine

The test engine was a JT15D 1 turbofan engine manufactured by Pratt and Whitney Aircraft of Canada, Ltd. The 21 in diam fan has 28 blades (see Fig. 1). The fan is followed by a stator assembly consisting of a bypass stator which has 66 vanes and a core stator which has 71 vanes. The latter is the only predominant difference between a production JT15D 1 engine (which has 33 core stator vanes) and the instrumented engine used in these tests. Because of the large number of both sets of vanes, rotor/bypass stator and rotor/core stator interactions are acoustically cut off over the engine operating range. The next rotating blade assembly is the compressor, which is a combination axial centrifugal compressor having 16 blades in the leading axial part of the unit.

As indicated in Fig. 1, the engine core is supported by six struts located in the intermediate case of the engine. These supports traverse both the compressor and bypass ducts to tie

Presented as Paper 83-0678 at the AIAA 8th Aeroacoustics Conference, Atlanta, Ga., April 11-14, 1983; received June 9, 1983; revision received Jan. 6, 1984. This paper is declared a work of the U.S. Government and therefore is in the public domain.

\*Aero Space Technologist, Noise Propagation Suppression Branch, Acoustic Noise Reduction Division, Member AIAA.

†Head, Noise Propagation Suppression Branch, Acoustic Noise Reduction Division.

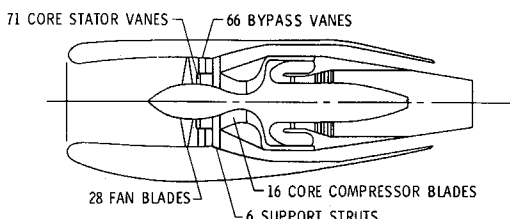


Fig 1 Cross sectional sketch of JT15D engine (with flight nacelle)

the core to the outer wall of the engine intermediate case. These struts are located directly behind the stator assembly.

Based on unpublished results provided by the Lewis Research Center, an inlet for the JT15D 1 engine was designed that would operate both at static and cruise conditions. Sketches showing dimensions of the inlet and major engine components may be found in Ref 14. Differences between static/tunnel/flight external nacelles and bypass duct acoustic treatments are also described in Ref 14.

#### Flight Test

##### Aircraft

Figure 2 shows a photograph of a modified OV 1 aircraft used to carry a JT15D engine for the flight tests. The JT15D engine was installed under the right wing at the pylon mount station which normally would carry the right auxiliary fuel tank.

Unpublished results from an array of hot film velocity sensors, flown in the position of the fuel tank prior to the installation of the JT15D, indicated that a significant velocity field induced by the rotating turboprop would be present and most likely produce an unwanted source of fan noise. Consequently, all flight testing was performed with the starboard turboprop shut down and feathered.

Based on an earlier wind tunnel test of the JT15D,<sup>12</sup> which incorporated an OV 1 wing and nonrotating turboprop, noise reflections and effects of installation were expected to be minimal in the far-field noise measurements.

##### Data Systems

Data were obtained from far field acoustic, aircraft tracking, meteorological, and onboard quasisteady and dynamic measurement systems.

Far field acoustic systems consisted of an array of microphones placed atop 30 ft poles situated on a runway at the Wallops Flight Facility. The microphones were condenser type pressure microphones (0.5 in diameter) fitted with grid caps and wind screens. They were oriented such that, as the airplane flew down the runway centerline, the engine passed directly over the microphones, thereby presenting a grazing incidence signal. There were eight microphones in all, each separated by 30 ft. Each microphone signal was amplified, high pass filtered at 1000 Hz, and recorded on a 14 channel wide band analog FM tape recorder. An IRIG A time code, synchronized with the other data systems, was also recorded.

The aircraft tracking system used to determine vehicle position consisted of an FPS-16 radar in conjunction with a colocated laser. The system focused on a laser reflector located in a fairing directly under the nose of the aircraft.

A meteorological system utilizing a helium filled tethered balloon was used to provide weather profiles before and during the flight tests. The instrumentation measured profiles of barometric pressure, wind direction and speed, temperature, and relative humidity from ground level to the aircraft flight altitude.

Onboard quasisteady aircraft and engine performance instrumentation, as well as fan blade fluctuating pressure measurement systems, are described in detail in Ref 15. Flight data on fan blade and stator vane pressures are presented in Refs 16 and 17, respectively.

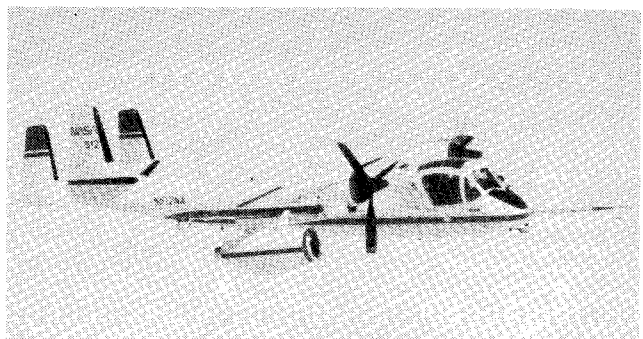


Fig 2 OV 1/JT15D flight configuration

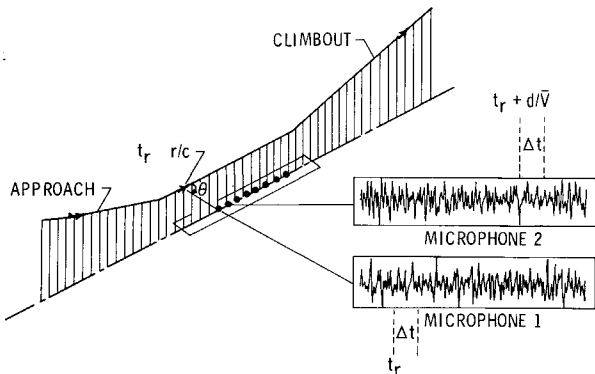


Fig 3 Flight operation and data reduction techniques

##### Operational Technique

Flight tests were performed at the NASA Wallops Flight Facility. A flight consisted of an aircraft flyover at a fixed JT15D power setting past the array of microphones located on the runway. The objective for the pilot was to hold the aircraft at constant altitude and constant velocity under trim conditions for the duration of the test interval (corresponding to acoustic emission angles of about 20 to 140 deg). Typically, the aircraft was flown at an altitude of 300 ft and an airspeed of 200 ft/s, resulting in an angle of attack between 3 and 9 deg. Sideslip and roll angles were nominally 0 deg.

##### Data Reduction

To study the nonstationary flyover process in a meaningful manner, a technique for analyzing the acoustic flyover data was developed. Details of the software methodology and computer programs can be found in Ref 18. The technique is as follows. First, the raw radar data was processed to provide time histories of range, elevation, and azimuth relative to the radar site. A transformation was applied to translate the origin of the coordinate system to the position of the first microphone in the linear array. Quasisteady onboard measurements of the aircraft attitude were then introduced to provide a six degree of freedom description of the position of the laser reflector relative to the first microphone. A linear transformation was applied to shift the data from the laser cube to the centerline of the inlet axis in the plane of the highlight. The data were now expressed in terms of a range  $r$  and angle  $θ$  from this engine reference point to the first microphone (see Fig 3).

To relate the information on the processed radar file to that on the acoustic tapes, the synchronized time code had to be adjusted for acoustic propagation time (retarded time). For a given acoustic recording time  $t_r$ , there was a corresponding engine emission time,  $t_e = t_r - r/c$ , where  $c$  is the average speed of sound as calculated from the meteorological tem-

**Table 1 Data adjustments for comparisons normalized to 100 ft radius, lossless, stationary conditions**

	Static	Tunnel	Flight
Instrumentation corrections	×	×	×
Inverse square law	×	×	×
Atmospheric absorption	×		×
Ground impedance	×		×
Convective amplification		×	×
Doppler frequency			×

perature profile. In this manner, the first microphone in the array was related to the noise emission angle. To maintain a high resolution of source location and, hence, emission angle, a time increment  $\Delta t$  of only 0.05 s was used in the fast Fourier transform process to obtain the narrowband acoustic spectra from the first microphone. A disadvantage of using short integration times, however, is poor estimation of the sound pressure level. To overcome this disadvantage, an ensemble averaging technique using multiple microphones was employed, that is, individual microphone spectra were averaged together based on identical aircraft to microphone emission angle. Since the microphones were spread out in a linear array under the flight path identical radiation angles occurred at times equal to  $t_r + (n-1)d/\bar{V}$  ( $d$  = the spacing between microphones and  $\bar{V}$  = the average speed of the aircraft over the array) for each of the  $n$  microphones in the array. In the present example, eight pole mounted microphones were ensemble averaged in this manner. This resulted in an angular resolution varying from 0.3 deg at shallow angles to 2.3 deg overhead and a chi squared 90% confidence value of about  $\pm 1$  dB for the sound pressure level. Spectra were calculated in 100 Hz bandwidth every 2 deg from 20 to 140 deg emission angle.

In the final step in the data reduction process, the flight narrowband acoustic spectra were adjusted to a static equivalent, 100 ft radius, atmospheric lossless reference condition using the measured radar and weather information. To do so required the application of the following considerations as listed in Table 1: 1) instrumentation corrections (Ref 19), 2) the inverse square law, 3) atmospheric absorption (Ref 20), 4) ground impedance (Ref 21), 5) convective amplification, and 6) Doppler frequency. The ground was assumed to be perfectly reflecting, which resulted in a 3 dB addition to the directly received noise signal over the frequency range of interest (> 1000 Hz). Convective amplification was assumed to be given by the factor  $-40 \log(1 - M_{ac} \cos \theta)$ , where  $M_{ac}$  is the Mach number of the aircraft. Directivity patterns relative to the inlet axis were generated by a computer program that tracked peaks in the ensemble averaged adjusted spectra. Often the acoustic energy was spread across two adjacent narrowbands which, because of Doppler smearing and the time delay between direct and reflected signals, had to be summed.

#### Wind Tunnel Test

Wind tunnel data used in the comparisons contained herein were obtained from tests in the NASA Ames 40 x 80 ft Wind Tunnel some of which have been previously reported in Ref 12. A description of the test setup, procedures, and a discussion of principal results can be found therein. A photo showing the test arrangement is presented in Fig. 4. Analog acoustic tape data were processed to yield 100 Hz narrowband spectra utilizing the same FFT program as was used in the flight data reduction. Adjustments to yield 100 ft radius, lossless conditions are indicated in Table 1.

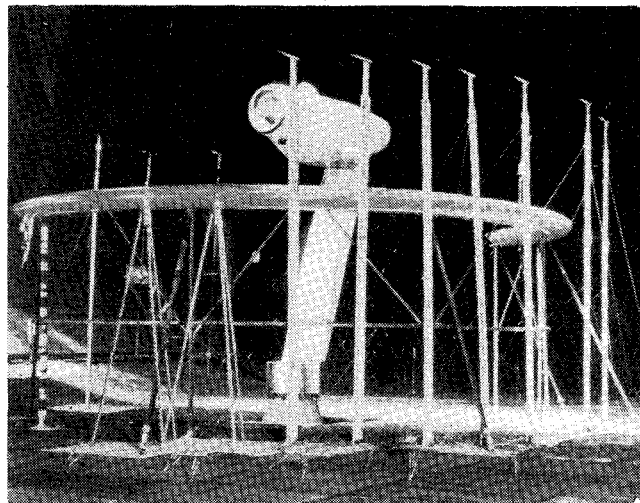


**Fig. 4 JT15D wind tunnel configuration**

#### Static Test

Static test stand data used in the comparisons were obtained from tests performed at the NASA Lewis Vertical Lift Facility (VLF). Data are presented for the JT15D engine utilizing the flight inlet lip both with and without an ICD. Construction details of the ICD, test setup description, and further acoustic results may be found in Refs 5 and 6. Analog acoustic tape data were also processed using the same FFT program as was used in the flight and tunnel data reduction procedures. Adjustments made to the static spectra are indicated in Table 1. Figure 5 shows the test engine at the VLF with ICD in place.

## Results and Discussion

#### Flowfield and Performance

As mentioned previously, the inlet of the JT15D was designed by personnel of the Lewis Research Center to operate over the range of test environments: static, wind tunnel, and flight. To validate the aerodynamic design various inlet flow conditions were exercised using an inviscid compressible potential flow computer program. Results showing vector flowfields and wall Mach number and pressure ratio distribution comparisons may be found in Ref 14. In general a quick recovery for all test environments was obtained with the inlet and near identical mean flowfield conditions existing at the fan face.

Other flowfield results based on measured data were: 1) a one per revolution circumferential distortion in the inlet of a magnitude greater than would be predicted by angle of attack induced distortion, 2) a slightly lower fan operating line in flight than for the static case, and 3) larger tip relative flow incidence angles for the static case at all fan speeds.

#### Far Field Acoustics

##### Separation of Components

The measured far field noise in flight contains all the JT15D noise sources as well as those from the OV 1. To separate the OV 1 component, all that was required was a flight test with the JT15D inoperative. A typical spectra comparing the JT15D/OV 1 at approach power with the OV 1 alone is shown in Fig. 6. Over the midpart of the spectra (between 2 and 9 kHz), there is a 5 to 20 dB signal to noise ratio. Around 1000 Hz and in the 10-11 kHz range the OV 1 spectra contaminates the JT15D noise field. JT15D jet noise and combustor noise have been determined<sup>22</sup> to peak at less than 1000 and 250 Hz respectively. These noise sources have been filtered out prior to the recording process. The fun-

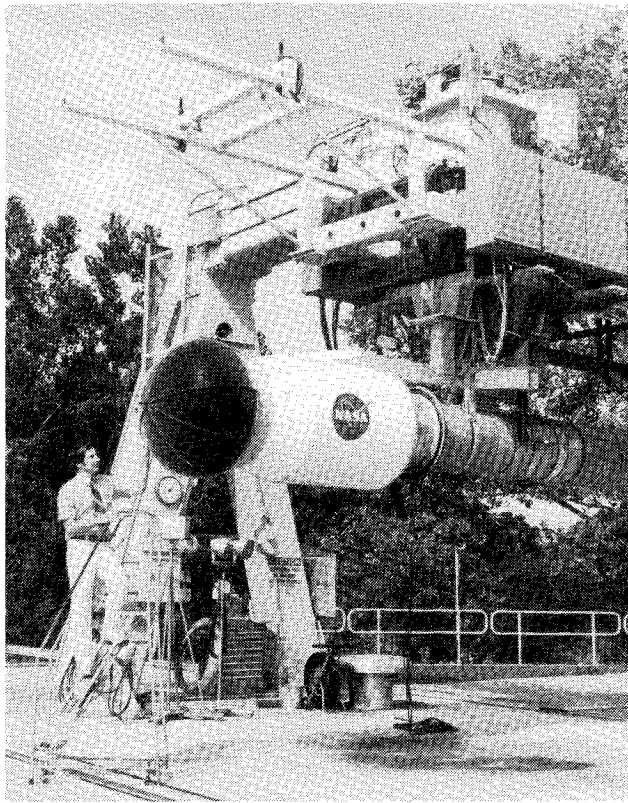


Fig. 5 JT15D static test configuration (with ICD).

damental fan tone occurs in the midfrequency range where the signal-to-noise ratio is high. The result in Fig. 6 corresponds to a radiation angle of 60 deg; similar results were found for all radiation angles of interest.

A question remaining in regard to the fan-noise data is: what exactly are the relative contributions of forward- and aft-radiated acoustic power? Deserving special consideration are the aft-radiated spinning modes well above cut-on which tend to radiate in the forward quadrant.<sup>23</sup> In order to separate forward- and aft-radiated fan noise, tests were conducted with and without inlet liners and with and without bypass duct noise suppressors. Both inlet and bypass liners utilized bulk absorber material for improved suppression bandwidth. Results are presented in Figs. 7a and 7b for subsonic and supersonic fan tip speeds, respectively. The two sets of data for hardwall inlets indicate that the bypass muffler was effective in reducing blade-passage-frequency tone noise at all angles aft of 80 deg. Testing the softwall inlet with the muffler in place was required to answer the question of whether aft-radiated noise was reduced sufficiently to make inlet noise dominant. The result is shown by the lower curve on both figures. Indeed, the softwall inlet greatly reduced the fan tone level for angles between 40 and 100 deg. Hence, it may be concluded that, for the hardwall inlet/bypass muffler case (the configuration to be studied in the remainder of this report), inlet-radiated fan noise dominated the forward arc. Subsequent results will be presented in the range from 0 to 90 deg.

#### Fan Noise Sources

For the JT15D the BPF tone has contributions from rotor-turbulence, rotor one-per-revolution distortion, rotor-potential field interaction, and from the rotor alone. Rotor-turbulence interaction<sup>2</sup> is the generally accepted mechanism dominating static testing with no ICD. The second two have been discovered to be major noise sources for the JT15D with ICD's at simulated forward speed and in flight based on

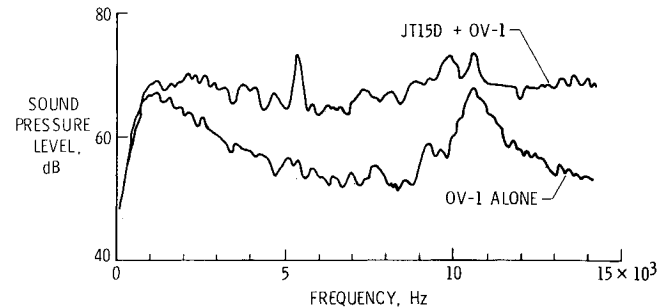
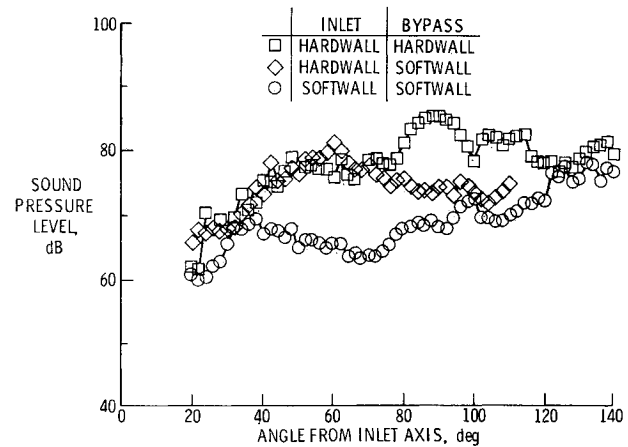
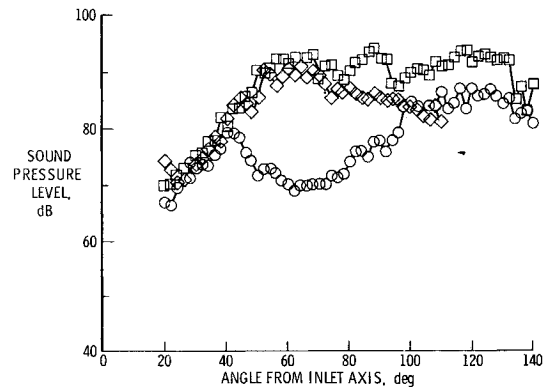


Fig. 6 Typical JT15D/OV-1 signal-to-noise ratio at 60 deg from inlet axis.



a) 10,800 rpm fan speed.



b) 13,500 rpm fan speed.

Fig. 7 Flight BPF tone directivity for various inlet and bypass duct wall configurations.

blade-mounted-transducer studies.<sup>5,12,16</sup> [Whereas the potential field interaction has been clearly identified with the six support struts (see Fig. 1), the one-per-revolution distortion has not been clearly identified.] Rotor-alone tone noise shows up at supersonic tip speeds and produces multiple-pure-tones (MPT's) at harmonics of the shaft rotational speed. As mentioned previously, rotor-stator interactions are cut off over the engine operating range.

The dominant practical mechanism of fan broadband noise generally remains an unknown. Rotor self noise<sup>24</sup> and rotor small-scale turbulence interaction have been postulated to produce broadband noise. The rotor tip interacting with the casing boundary layer may be a major contributor to broadband noise.<sup>25</sup> The highest relative velocities and the highest inflow turbulence levels are present there.

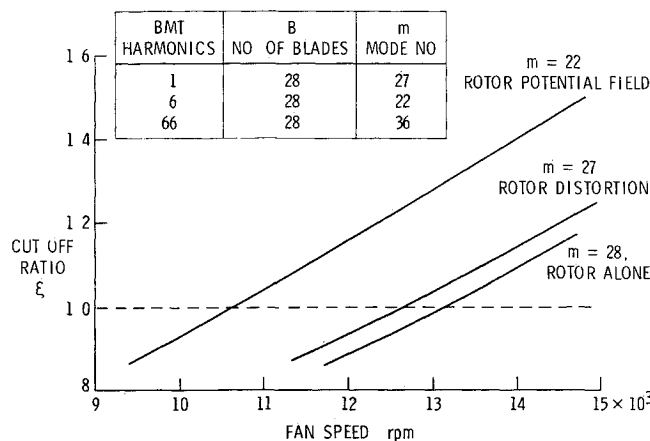


Fig 8 Cut off ratio for several modes

The relative contributions of fan noise source mechanisms to the blade passage frequency tone and broadband noise level depend in general on fan speed and the radiation directivity angle, as well as the test configuration (with/without ICD) and test environment (static/tunnel/flight). The degree to which they contribute will be addressed in a later section of this paper. To aid in understanding the contributions of fan tone noise mechanisms at various fan speeds, the Tyler Sofrin cut off ratio for selected modes is presented in Fig 8. The dominant BMT harmonics<sup>16</sup>  $V$  of 1, 6, and 66 result in rotor one per revolution distortion, rotor strut potential field, and rotor bypass stator interactions. Since there are 28 fan blades,  $B$ , these interactions produce acoustic spinning modes ( $m = B - V$ ) of circumferential order 27, 22 and -38 respectively. The criterion for propagation to the far field is the cut off ratio  $\xi$  given by

$$\xi = \frac{BM_t}{k'_{m,\mu} (1 - M^2)^{1/2}}$$

where  $M_t$  and  $M$  are the rotor tip and duct flow Mach number, respectively, and  $k'_{m,\mu}$  is the mode eigenvalue for a cylindrical duct. A given mode will propagate down the duct if  $\xi > 1$  and will decay exponentially if  $\xi < 1$ . Thus it is seen from Fig 8 that the  $m = 22$  mode will be above the cut off point at fan speeds greater than 10 650 rpm and the  $m = 27$  mode at speeds greater than 12 750 rpm. The rotor stator interaction is below cut off over the operating range of interest. A rotor alone mode ( $m = 28$ ), which has a cutoff point at 13,200 rpm, is also shown.

#### Accuracy and Repeatability

The degree to which effective data comparisons can be made depends largely on the accuracy and repeatability of the flight test data. Figure 9 presents flight data at a 60 deg emission angle and an approach power setting which compare a single microphone spectra and an ensemble averaged, static equivalent adjusted spectra. Ensemble averaging causes a smoothing in the spectra and a clear enhancing of the coherent parts of the signal, namely, the tones. Adjusting to a static equivalent condition changes both the level and the shape of the spectra. Note the large adjustment at high frequencies due chiefly to the characteristics of atmospheric absorption. Chi squared 90% confidence levels are -4.7 to +2.9 dB for the single microphone result and -1.4 to +1.2 dB for the multi microphone result. This represents a significant improvement in the accuracy of the tone levels.

Repeatability of the tone level directivity was studied by conducting flight tests at near identical power settings (13,400  $\pm$  25 rpm) on different days from two flight test series: one in

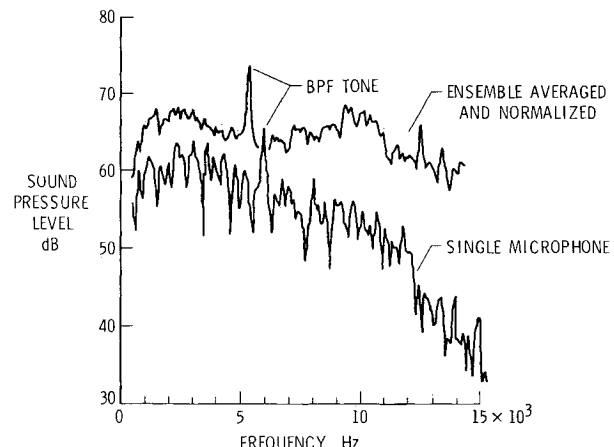


Fig 9 Typical flight spectra comparison at 60 deg from inlet axis for an approach power setting

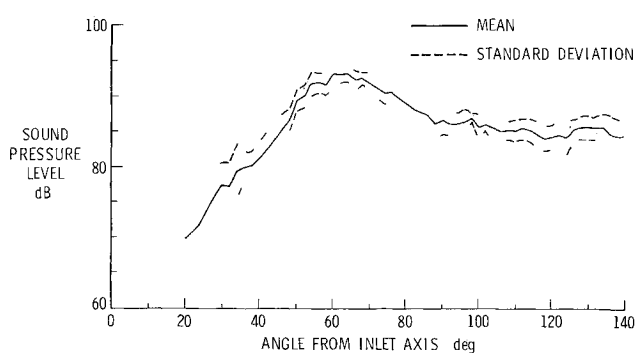


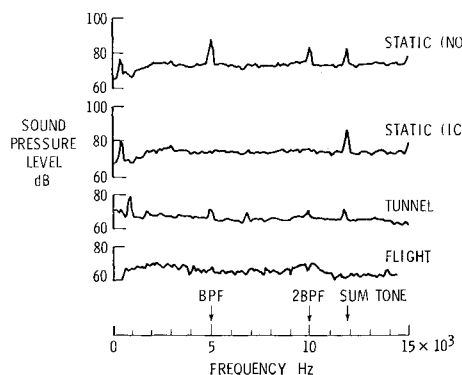
Fig 10 Variability of BPF tone directivity for six flights at near identical fan speeds

the fall of 1980, the other in the summer of 1981. Results incorporating data from six such flight tests are presented in Fig 10. The mean and standard deviation for the blade passage frequency tone are shown as a function of emission angle. The standard deviation ranges from about  $\pm 4$  dB at 20 deg to about  $\pm 2$  dB near the peak radiation angle and overhead. These variations are slightly greater than the statistical accuracy stated for the ensemble averaged spectra and are most likely due to the imprecise representation of the atmosphere used in the data reduction process. The atmosphere was modeled by a single weather balloon system near the microphone array and assumed to be homogeneous and quiescent in each layer. No account was taken for refraction by wind and temperature gradients or scattering by turbulence. In addition, some variations might have been due to the noise source (as determined by power setting) not being exactly the same for each flyover, although care was taken to minimize this.

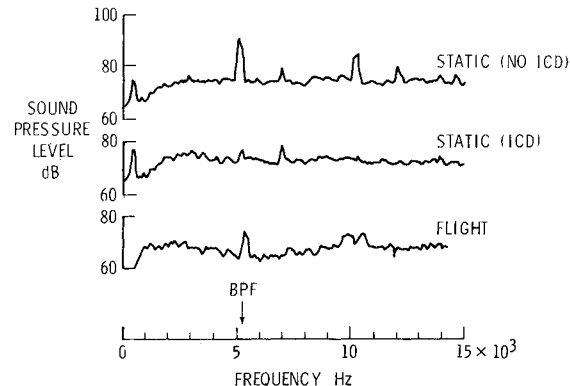
#### Comparisons

Static (with and without ICD) wind tunnel and flight far field acoustic data will be compared on the basis of static equivalent atmospheric lossless conditions at a constant radius of 100 ft. Comparisons are made for power settings representative of subsonic, transonic, and supersonic tip speeds.

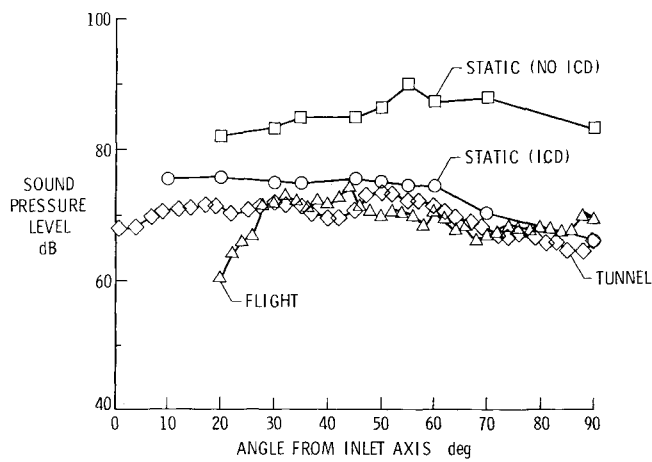
Figures 11a and 11b present both comparisons of narrowband spectra (100 Hz) at an inlet emission angle of 60 deg and directivity plots of the sound pressure level in the band where the blade passage frequency (BPF) would be present. In general, all spectra are relatively flat across the frequency range. Corrected fan speed is within 0.5% of 10 500 rpm for all cases. The static (no ICD) data reveals a



a) Spectra at 60 deg from inlet axis



a) Spectra at 60 deg from inlet axis

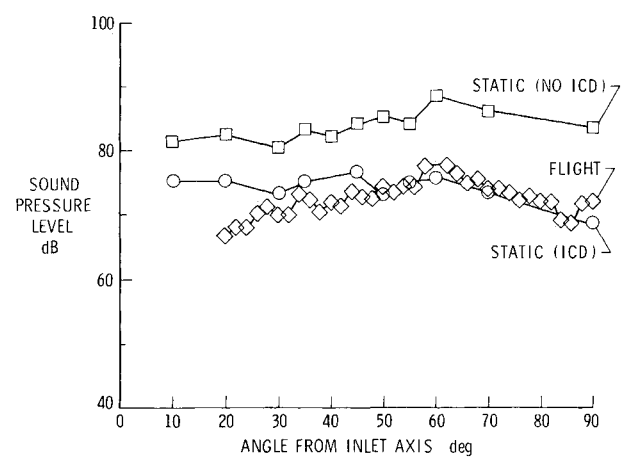


b) BPF tone directivity

Fig 11 Data comparisons at 10,500 rpm fan speed

sizeable tone at the blade passage frequency of about 5000 Hz. The addition of the ICD reduces the tone level below the broadband floor. This result, as demonstrated in several other references and most recently in Ref 6, can be attributed to the lessening of the interaction between the rotor and unsteady inflow distortions such as turbulence, ground vortices and test stand wakes. Note that twice the blade passage frequency (2 BPF) tone is also reduced by the ICD, suggesting that this tone is also inflow related as opposed to being a rotor stator interaction (which is above cut off at this fan speed). A sum tone at 11.8 kHz involving the core compressor is relatively unaffected, however. The tunnel spectra (100 ft/s tunnel speed) reveals a residual tone at the BPF, while no tone is evident for the flight spectra. It was shown in Fig 8 that at this particular fan speed, the rotor strut potential field interaction ( $m = 22$ ) is near cut off. It is believed that the tunnel tone is due to this interaction rather than residual rotor turbulence interaction. As was discussed in Ref 12 rotor turbulence interaction in the tunnel is predicted to be nearly 10 dB below the level shown here.

The directivity patterns displayed in Fig 11b reveal the "across the board" nature of the ICD noise reduction. The ICD result is several dB higher than tunnel and flight but this is due to the broadband floor being higher and not due to the inability of the ICD to reduce the BPF tone level. The flight result shows a sudden drop in level forward of a 30 deg radiation angle. It is not known whether this is a real flight effect that was not simulated by the wind tunnel or ICD or if there exists an inadequacy in the adjustment process for the flight data. At shallow angles, the adjustments are large in magnitude. At 20 deg for example convective amplification



b) BPF tone directivity

Fig 12 Data comparisons at 10,800 rpm fan speed

was  $-4.3$  dB, inverse square law was 22.8 dB, and at atmospheric absorption was 11.9 dB. In addition flowfield differences in the inlet lip region, as discussed in Ref 14, were not accounted for in making the comparisons.

Figures 12a and 12b present spectra and directivity comparisons for static and flight data at a slightly higher (but still subsonic) fan speed of 10,800 rpm. At this fan speed the  $m = 22$  mode is well above cut off and a BPF tone is present for all cases. Tunnel runs were not made at this fan speed. Again results show the ICD effectiveness in reducing the BPF level at all angles, the excellent agreement between ICD and flight directivities aft of 30 deg, and lower broadband noise levels experienced in flight.

Broadband noise comparisons between flight and static ICD at a subsonic fan speed are presented in Fig 13. Reference 24 suggests the peak broadband noise occurs in the one third octave band about two and one half times the blade passage frequency. For the present flight data this would not only be in a frequency range where the OV 1 background noise contaminates but, also, where the atmospheric absorption adjustment is extremely high. Hence it was convenient to define the broadband level to be the level at the base of the BPF tone. Since the spectra are nearly flat to begin with, this choice seemed reasonable enough. As indicated previously the static data shows higher broadband levels at all angles. Also shown on the figure is an estimated flight directivity accounting for the tip incidence angle difference as reported in Ref 14. The adjustment which is an additional adjustment beyond those listed in Table 1, was taken to be 2.1 dB per degree (an average value from Refs 24 and 25). The adjustment was arbitrarily assumed to apply at all radiation

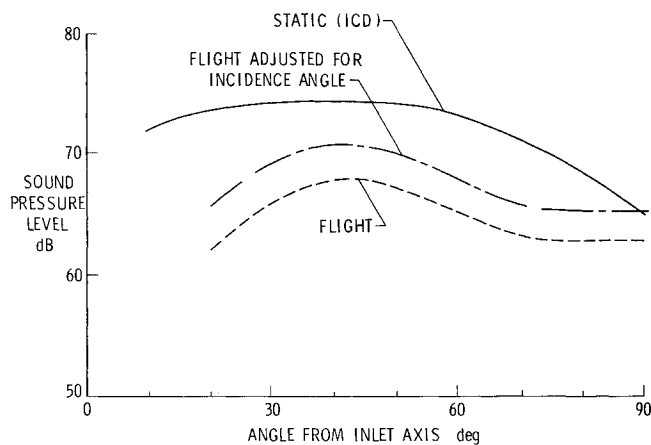


Fig. 13 Broadband noise comparison at 10,500 rpm fan speed

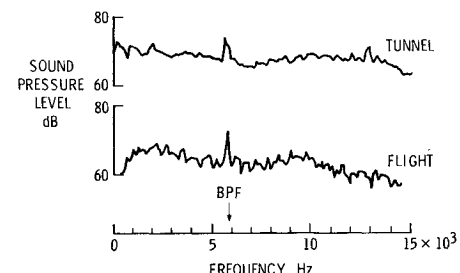
angles. It is seen in Fig. 13 that this adjustment accounts for part of the static flight difference. The remaining difference is not accounted for, although it is realized that corrections for incidence are based on mean flow considerations near the wall while in actuality there are most likely some differences in thickness and turbulence intensity in the boundary layer between static and flight.

No broadband comparisons are made for supersonic tip speeds since the broadband level is masked by buzzsaw noise.

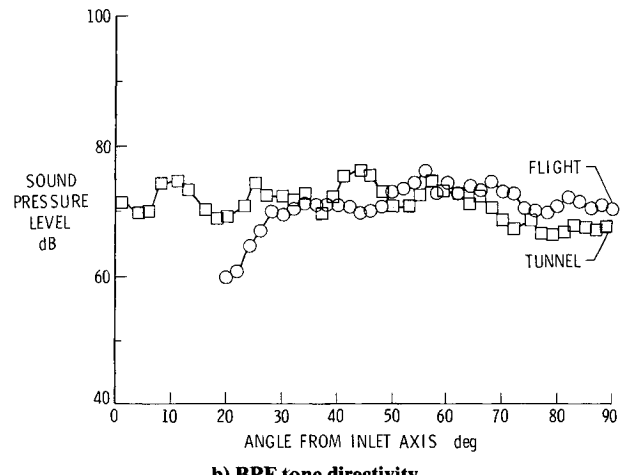
Spectral and directivity comparisons are made between wind tunnel and flight at a corrected fan speed of 11,900 rpm and are presented in Figs. 14a and 14b. This fan speed results in a transonic tip speed Mach number of 1.04. Blade passage frequency tone levels are nearly identical in the spectra of 60 deg. However, as in the case with the static data, the broadband noise level is higher in the tunnel than in flight. Inlet static pressure data, from which incidence angle is derived, was not available during the tunnel runs, so corrections cannot be made. Also, it was not known if the engine was on the proper operating line. Nevertheless, the broadband difference is about 4 dB between 1 and 10 kHz, which is much smaller than the static flight uncorrected difference of about 8 dB at this radiation angle.

The directivity comparison reveals a similarity in level except for angles less than 30 deg where the flight data again are considerably low. The tunnel data have several distinct peaks which have been attributed to inlet radiation of several duct radial modes related to the rotor strut potential field interaction.<sup>12</sup> This effect is not clearly delineated in the flight data, possibly due to a smearing effect resulting from aircraft motion and long range propagation.

Acoustic spectra from fans operating at supersonic tip speeds are dominated by multiple pure tones (MPT's). MPT's are generated as a direct result of small amplitude variations in the blade attached shocks due to normal manufacturing tolerances. These shocks propagate at different speeds creating shock interval variations forward of the fan. The interval variations show up as multiple tones of the engine shaft speed in the far field acoustic spectra. Since fan irregularities due to manufacturing tolerances are not exactly duplicated, the MPT spectra from fans of the same design will be different. For this reason, the same fan used in the earlier static tests was flight tested over a range of supersonic tip speeds. A comparison between flight and static spectra at a radiation angle of 60 deg for a supersonic tip fan is presented in Fig. 15. Corrected fan speed was about 13,540 rpm; all data were within  $\pm 20$  rpm of that value. Static test results with and without ICD are nearly identical. This was expected since the ICD should have no effect on this noise source mechanism. The flight spectra show some similarity. A strong BPF tone occurs near 6400 Hz and the MPT harmonics cluster around 4000 Hz. However, the details describing the level of acoustic



a) Spectra at 60 deg from inlet axis



b) BPF tone directivity

Fig. 14 Data comparisons at 11,900 rpm fan speed

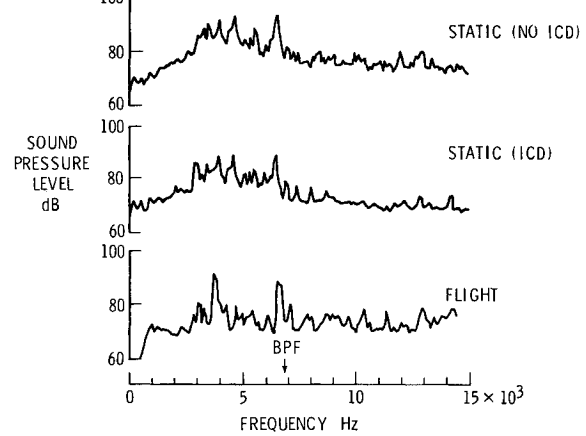


Fig. 15 Spectra comparison at 60 deg from inlet axis and 13,500 rpm fan speed

energy in each narrow band are markedly different. The possibility of a "flight effect" on MPT noise has been suggested in Ref. 4 and seems to be further supported here. It should be noted that, although the identical fan was operated at the same fan speed for both static and flight cases, tip relative Mach number was different. An additional flight test series was conducted to study the effect of tip Mach number. Results of this test series are presented in Fig. 16. At a calculated tip relative Mach number of 1.09 (corrected fan speed of 12,570 rpm) a strong BPF tone is present but there is no evidence in the far field of MPT's. At this fan speed only the  $m=22$  mode is above cut off. Both rotor one per revolution distortion ( $m = 27$ ) and rotor alone ( $m = 28$ ) are cut off. At a tip Mach number of 1.16 (13,300 rpm), all of the

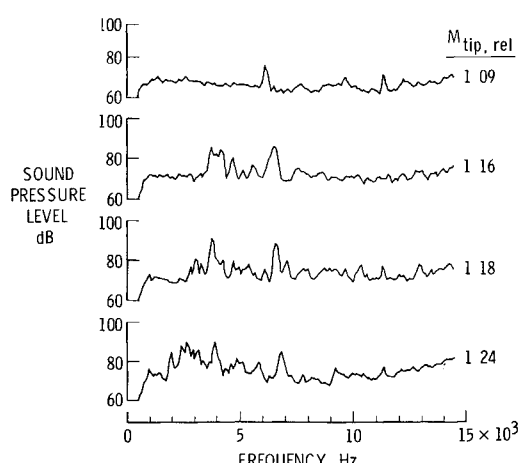


Fig 16 Flight spectra comparison at 60 deg from inlet axis for various tip relative Mach numbers

above modes are above cut off, the BPF tone level rises 10 dB and MPT's are present. At a slightly higher Mach number of 1.18 (13 540 rpm), the distribution of MPT power shifts among the various narrowbands. This is further evidenced at a Mach number of 1.24 (14 180 rpm) where there is a shift of MPT power to the lower frequency bands. Hence it appears that a precise matching of fan tip Mach number may be required in order to critically evaluate the question of the existence of flight effects on multiple pure tone noise.

Figure 17 presents static wind tunnel, and flight comparisons for the BPF tone integrated over the forward hemisphere. Results are shown in terms of a relative sound power as a function of corrected fan speed. The flight data show an increasing sound power level with fan speed consistent with the cut off point of certain spinning modes as illustrated previously in Fig 8. The static data without an ICD is on the order of 10 dB higher than the flight data at moderate fan speeds (<12,000 rpm) where the fan tip relative Mach number is subsonic and rotor turbulence interaction dominates the noise field. The addition of an ICD reduces the sound power to a level consistent with the flight and wind tunnel levels. At high fan speeds where the fan tip relative Mach number is supersonic, rotor alone noise is a major noise mechanism and the ICD has little effect. But here again, good agreement exists with the flight results.

### Conclusions

A flight test program utilizing a JT15D 1 turbofan engine has been conducted with the objective of studying flight effects on fan noise and evaluating the simulation effectiveness of both a wind tunnel and a static test configuration that incorporates an inlet control device (ICD). In conjunction with synchronized laser radar tracking and meteorological profile information, a linear array of ground microphones was narrowband analyzed and ensemble averaged to yield highly accurate far field acoustic results. Utilizing instrumentation corrections convective amplification, spherical spreading, atmospheric absorption, ground impedance, and Doppler frequency considerations where appropriate all three sets (flight, static, wind tunnel) of data were normalized to static equivalent 100 ft radius, lossless conditions.

Data comparisons resulted in the following conclusions:

1) For the fan operating subsonically, the use of an ICD during static tests was effective in reducing the BPF tone to a level comparable to flight. Good agreement was obtained at all radiation angles except forward of 30 deg where the flight data dropped off rapidly. It could not be ascertained if the shallow angle difference was due to an inadequacy in any of

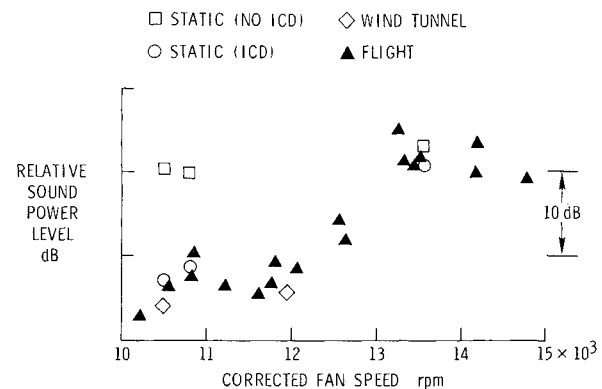


Fig 17 Relative BPF tone sound power comparison

the normalization elements (e.g., convective amplification) to different refraction effects in the inlet lip region or to some other unknown effect.

2) Good agreement was obtained between wind tunnel and flight BPF tone levels at subsonic and transonic fan speeds, except at shallow angles where the flight levels were lower again. In addition in the tunnel the transonic fan directivity revealed a multilobed structure suggesting discrete spinning modes, whereas in flight no such structure was evident.

3) Flight noise source mechanisms suggested by fan blade mounted pressure transducer measurements<sup>16</sup> were supported by far field acoustic results. A tone (100 Hz narrowband) was first observed in flight near cut off of a rotor potential field interaction noise source. Further increases in tone level occurred near cut on of rotor one per revolution distortion and rotor alone mechanisms.

4) Broadband noise levels in flight were about 3 to 10 dB lower than in static tests depending on radiation angle. Part of the difference was accounted for when a correction was made for differences in fan blade flow incidence angle. The remaining difference was not accounted for.

5) Multiple pure tone noise in flight was found to be very sensitive to changes in tip relative Mach number. Static and flight comparisons made with the same rotor at essentially the same corrected fan speed but different tip Mach number revealed differences in the narrowband content of the various shaft harmonics. The possibility of a "flight effect" on MPT noise remains.

### References

- Cumpsty N A and Lowrie B W 'The Cause of Tone Generation by Aero Engine Fans at High Subsonic Tip Speeds and the Effect of Forward Speed' ASME Paper 73 WA/GT 4 Nov 1973
- Hanson D B 'Spectrum of Rotor Noise Caused by Atmospheric Turbulence' *Journal of the Acoustical Society of America* Vol 56 No 1 July 1974, pp 110-126
- Ho P R Smith, E B and Kantola R A 'An Inflow Turbulence Reduction Structure for Scale Model Fan Testing' AIAA Paper 79 0655 March 1979
- Atvars Y and Rogers D F 'The Development of Inflow Control Devices for Improved Simulation of Flight Noise Level During Static Testing of a HBPR Turbofan Engine' AIAA Paper 80 1024 June 1980
- McArdle J G Jones W L Heidelberg L J, and Homyak L 'Comparison of Several Inflow Control Devices for Flight Simulation of Fan Tone Noise Using a JT15D 1 Engine' NASA TMX 81505 June 1980
- Homyak L McArdle J G and Heidelberg, L J, 'A Compact Inflow Control Device for Simulating Flight Fan Noise' AIAA Paper 83 0680 April 1983
- Peracchio A A Ganz, U and Gedge M 'Studies on Proper Simulation During Static Testing of Forward Speed Effects on Fan Noise' NASA CR 165626 Sept 1980
- Falarski, M D and Moore, M T, 'Acoustic Characteristics of Two Hybrid Inlets at Forward Speed' *Journal of Aircraft* Vol 17 Feb 1980 pp 106-111

- <sup>9</sup>Ahtye W F A Measurement of Forward Flight Effects on the Noise from a JT15D 1 Turbofan Engine in the NASA Ames 40 x 80 Foot Wind Tunnel AIAA Paper 80 1026 June 1980
- <sup>10</sup>Moore M T Forward Velocity Effects on Fan Noise and the Suppression Characteristics of Advanced Inlets as Measured in the NASA Ames 40 x 80 Foot Wind Tunnel NASA CR 152328 Sept 1979
- <sup>11</sup>Holm R G Langenbrunner L E and McCann E O, Forward Velocity Design as Measured in the NASA Ames 40 x 80 Foot Wind Tunnel NASA CR 152329, July 1981
- <sup>12</sup>Preisser J S Schoenster J A Golub R A and Horne C Turbofan Engine Blade Pressure and Acoustic Radiation at Simulated Forward Speed *Journal of Aircraft* Vol 20 April 1983 pp. 289 297
- <sup>13</sup>Rogers D F and Ganz U W Aerodynamic Assessment of Methods to Simulate Flight Inflow Characteristics During Static Engine Testing AIAA Paper 80 1023 June 1980
- <sup>14</sup>Golub R A and Preisser, J S Development and Test Engine/Inlet Performance of a Vehicle for Flight Effects on Fan Noise Research NASA TP 2254, April 1983
- <sup>15</sup>Knight, V H Jr "In Flight Jet Engine Noise Measurement System" Presented at the ISA 27th International Instrumentation Symposium April 1981
- <sup>16</sup>Schoenster J A Fluctuating Pressure Measurements on the Fan Blades of a Turbofan Engine During Ground and Flight Tests
- AIAA Paper 83 0679 April 1983
- <sup>17</sup>Mueller A W Study of Stator Vane Fluctuating Pressures in a Turbofan Engine for Static and Flight Test NASA TP 2217 April 1983
- <sup>18</sup>Gridley D, Program for Narrow Band Analysis of Aircraft Flyover Noise Using Ensemble Averaging Techniques NASA CR 165867 March 1982
- <sup>19</sup>Mueller A W A Comparison of the Three Methods Used to Obtain Acoustic Measurements for the NASA Flight Effects Program NASA TM 81906 1980
- <sup>20</sup>American National Standard Method for the Calculation of the Absorption of Sound by the Atmosphere American National Standards Institute Inc ANSI S1 2 1962 (R1971) Aug 1962
- <sup>21</sup>Acoustic Effects Produced by a Reflecting Plane Society of Automotive Engineering, AIR 1327 Jan 1976
- <sup>22</sup>Reshotko, M and Karchmer A Core Noise Measurements from a Small General Aviation Turbofan Engine NASA TM 81610 April 1980
- <sup>23</sup>Rice E J and Saule, A V Farfield Radiation of Aft Turbofan Noise NASA TM 81506, April 1980
- <sup>24</sup>Ginder R B and Newby D R, An Improved Correlation for the Broadband Noise of High Speed Fans *Journal of Aircraft* Vol 14, Sept 1977 pp 844 849
- <sup>25</sup>Gliebe, P R The Effect of Throttling on Forward Radiated Fan Noise ' AIAA Paper 79 0640 March 1979.

*From the AIAA Progress in Astronautics and Aeronautics Series*

**AERO-OPTICAL PHENOMENA—v. 80**

*Edited by Keith G Gilbert and Leonard J Otten Air Force Weapons Laboratory*

This volume is devoted to a systematic examination of the scientific and practical problems that can arise in adapting the new technology of laser beam transmission within the atmosphere to such uses as laser radar laser beam communications laser weaponry and the developing fields of meteorological probing and laser energy transmission among others The articles in this book were prepared by specialists in universities industry and government laboratories both military and civilian, and represent an up-to date survey of the field

The physical problems encountered in such seemingly straightforward applications of laser beam transmission have turned out to be unusually complex A high intensity radiation beam traversing the atmosphere causes heat up and break down of the air changing its optical properties along the path so that the process becomes a nonsteady interactive one Should the path of the beam include atmospheric turbulence, the resulting nonsteady degradation obviously would affect its reception adversely An airborne laser system unavoidably requires the beam to traverse a boundary layer or a wake with complex consequences These and other effects are examined theoretically and experimentally in this volume

In each case, whereas the phenomenon of beam degradation constitutes a difficulty for the engineer it presents the scientist with a novel experimental opportunity for meteorological or physical research and thus becomes a fruitful nuisance!

412 pp 6 x 9 illus \$30 00 Mem \$45 00 List

TO ORDER WRITE: Publications Order Dept AIAA 1633 Broadway New York N Y 10019